

Facile sonochemical assisted synthesis of Cu₂O and CuO nanoparticles

B.Sathish Mohan^a, Dharmasoth Ramadevi^b, K.Basavaiah^{a,*}

^a Department of Inorganic and Analytical Chemistry, Andhra University, Visakhapatnam-530003, India

^b AU College of Pharmaceutical Sciences, Andhra University, Visakhapatnam-530003, India

ARTICLE INFO

Article history:

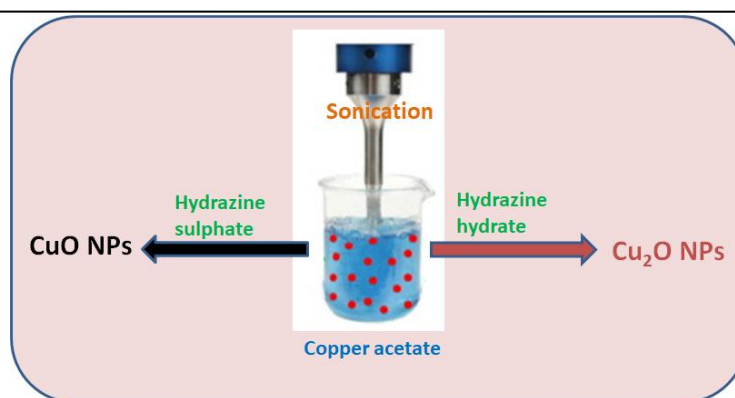
Received: 06 January 2019

Accepted: 28 June 2019

Available online: 31 July 2019

Manuscript ID: PCBR-1901-1013

GRAPHICAL ABSTRACT



KEYWORDS

CuO NP
Cu₂O NP
Hydrazine hydrate/sulphate
Sonochemical
DRS

ABSTRACT

This work reports on cupric oxide (CuO) nanoparticles (NPs) and cuprous oxide (Cu₂O) NPs synthesized using facile green sonochemical method. Phase analysis, morphology, and crystallinity of the prepared NPs were investigated using X-ray diffraction (XRD), Fourier transform infrared (FTIR), field emission scanning electron microscopy (FESEM), energy dispersive X-ray (EDS), and UV-visible diffuse reflectance spectroscopy (DRS). The phase of NPs was tuned as a function of reducing agents. XRD patterns confirmed the presence of pure CuO NPs and Cu₂O NPs. FTIR peak at 621 cm⁻¹ confirmed Cu(I)-O vibrations, while CuO vibrations confirmed by the presence of two peaks at 536 and 586 cm⁻¹. The FE-SEM results showed that the morphology of the CuO NPs and Cu₂O NPs was highly uniform. EDS confirmed the elemental composition of Cu and O in both CuO NPs and Cu₂O NPs.

1. Introduction

Over the last two decades, functional nanomaterials have received great attention for many technological applications including, catalysis, energy, environment, medical, and sensor due to their unique properties at nanoscale [1-5]. Especially, transitional metal/metal oxides nanoparticles (NPs) based materials have attracted much attention due to their unique optical, magnetic,

electronic, and catalytic properties [6, 7]. Among these, copper oxides NPs such as CuO NPs and Cu₂O NPs have most widely investigated for many potential applications such as ultraviolet and/or visible light-driven photocatalysis, anti-oxidant, anti-fungal, smart windows, IR detector, gas sensors, batteries, high temperature superconductors and optical limiters [8-11] due to their wide bandgap, high TC, high optical absorption and non-toxic in nature. The physical and chemical properties of

* Corresponding author: Tel: 09908036203
E-mail: klbasu@gmail.com
†Electronic Supplementary Information (ESI) available

CuO NPs and Cu₂O NPs are depend on their size, morphology, and phase purity. Therefore lots of efforts have been taken to prepare pure CuO NPs and Cu₂O NPs with different morphology and size. So far, numerous methods are sonochemical preparation, alkoxide-based preparation, microwave irradiation, precipitation pyrolysis and thermal decomposition [12, 13].

In the present work, we report the synthesis of the pure CuO NPs and Cu₂O NPs using copper acetate as a precursor by varying the reducing agents hydrazine sulphate and hydrazine hydrate via sonochemical method.

2. Materials and Methods

Copper acetate [Cu(CH₃COO)₂ H₂O], sodium hydroxide (NaOH), hydrazine sulphate (N₂H₄ H₂SO₄) and hydrazine hydrate (N₂H₄ H₂O) were used as received from Merck chemicals, India. Milli Q water was used throughout all synthesis process. All the chemicals were of Analytical grade and used without further purification.

2.1 Synthesis of CuO NPs and Cu₂O NPs

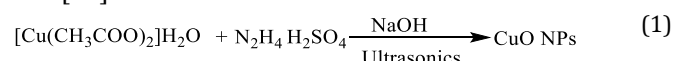
In order to synthesis Cu₂O NPs, 100 mL of 0.25 M [Cu(CH₃COO)₂ H₂O] was ultrasonicated for 10 min, then 100 mL of 0.1 M NaOH was added to the above solution. The reaction mixture was ultrasonicated further for 20 min, then 1M hydrazine hydrate was added drop wise. Afterwards, the reaction system was exposed to high-intensity ultrasonic irradiation powers under ambient air for 30 min. The reddish precipitate was formed and centrifuged, washed periodically with distilled water and absolute ethanol, then dried under vacuum at 60 °C. The same procedure has been adopted to preparation of CuO NPs using hydrazine sulphate as reducing agent. The black colour precipitate was dried under vacuum at 60 °C.

2.2 Instrumentation

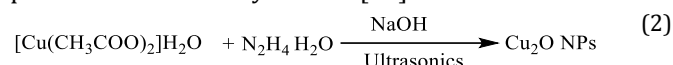
X-Ray diffraction (XRD) with Cu K α radiation at 30.0 kV and 30.0 mA over the scan range 2 θ , 10-800 at the scan rate of 20 min⁻¹ for the diffraction peaks were recorded. FTIR (IR Prestige 21, Shimadzu, Pvt Ltd, Japan) spectra of the samples in KBr pellets were obtained on a Shimadzu spectrometer in the range of 500-3600 cm⁻¹. Morphology of the as-prepared NPs was investigated field emission scanning electron microscopy (FE-SEM, model JSM-6610LV, Jeol Asia PTE Ltd, Japan.) equipped with the energy dispersive X-ray spectroscopy (EDS) analysis. UV-Visible diffuse reflectance spectra were recorded by UV-Visible diffuse reflectance spectrometer (Shimadzu, model 2600R).

3. Results and Discussion

Pure CuO NPs and Cu₂O NPs phase were prepared by sonochemical assisted method using copper acetate as precursor by varying the reducing agent with high intensity ultrasonics (vibracell, 20 kHz, 50 % amplitude and 100 W/cm²) for 1 h. The reducing agent has played very crucial role in the formation of phase purity of CuO NPs and Cu₂O NPs. The CuO NPs were obtained through copper acetate reacts with hydrazine sulphate and sodium hydroxide undergoes sonication (Equation 1). Due to the abundance of OH⁻ ions copper acetate was formed the resulting product is black, confirmed the formation of CuO NPs [14].



Similarly, the Cu₂O NPs were obtained through copper acetate reacts with hydrazine hydrate and sodium hydroxide undergoes sonication (Equation 2). These Cu₂O NPs were formed through the Cu²⁺ ions are reduced to Cu⁺ by hydrazine hydrate as reducing agent in the presence of sodium hydroxide [15].



The overall chemical reaction occurring in sonochemical synthesis of Cu₂O can be written as given in equations (3-9) [16].

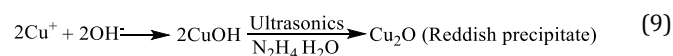
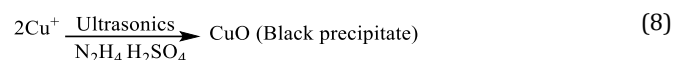
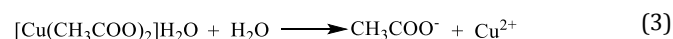


Figure 1 displays the XRD patterns of the CuO NPs and Cu₂O NPs. Figure 1a shows the XRD patterns for the precursor (copper acetate) sonicated in presence of reducing agent, hydrazine sulphate. The strong diffraction patterns at 2 θ =35.60 and 38.80 were indexed as [002] and [111] planes of monoclinic CuO NPs (JCPDS File No: 45-0937). Figure 1b shows the diffraction peaks centered at 2 θ = 36.680, 42.60, 61.760, 73.980 and 77.80 were attributed to (111), (200), (220), (311), and (222) orientation plane of Cu₂O with a cubic phase (JCPDS File No: 5-669). There were no impurity peaks were observed

for CuO NPs and Cu₂O NPs. The average crystallite size of both CuO NPs and Cu₂O NPs were calculated by Debye-Scherrer equation (10) and found to be 27.62 and 24.38 nm respectively.

$$D = 0.9\lambda / (\beta \cos\theta) \tag{10}$$

Where λ is the wavelength of X-ray radiation and β is the full width at half maximum of the peaks at the diffracting angle θ .

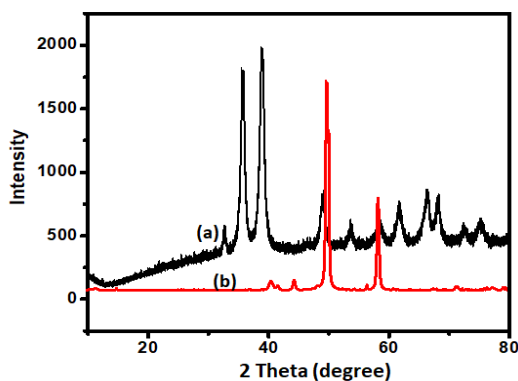


Fig. 1. XRD patterns of prepared CuO NPs (a), and Cu₂O NPs (b)

FTIR spectra of CuO NPs and Cu₂O NPs were presented in Figure 2. The two characteristic peaks (Figure 2a) at 586 cm⁻¹ and 536 cm⁻¹ were due to the Cu(II)-O stretching vibrations confirms the formation of CuO NPs [17, 18]. The characteristic peak at around 621 cm⁻¹ is attributed to the Cu(I)-O stretching vibrations in Cu₂O NPs [Figure 2b].

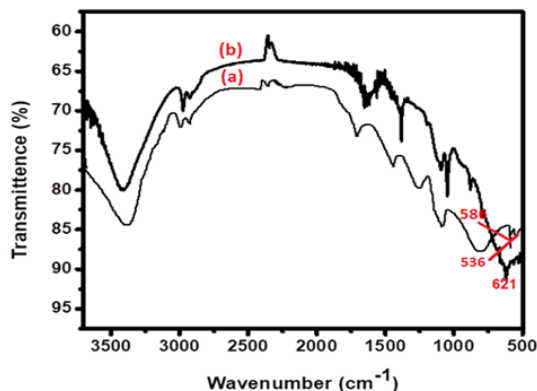


Fig. 2. FTIR spectra of a) CuO NPs and b) Cu₂O NPs

The bandgap of as-prepared CuO NPs and Cu₂O NPs were estimated by UV-Visible DRS (Figure 3) and bandgap was calculated using Equation 11.

$$E_g = h\nu = hc/\lambda = 1240/\lambda \tag{11}$$

where E_g is bandgap energy, h is planks constant, ν is wave frequency, c is the speed of light and λ is the wavelength. It can be seen that the Cu₂O has an absorption

edge around 681 nm corresponding to the bandgap of 1.82 eV [19]. However, the CuO indicated optical absorption for a wide range of wavelength at 521 nm. It is known that CuO has a wide range of band gaps in 2.38eV [20].

The representative FESEM images of CuO NPs and Cu₂O NPs were presented in Figure 4. The morphology of CuO NPs rod like structure (Figure 4 (a,b)) while the morphology of Cu₂O NPs was found to be octahedral like structure (Figure 4 (c,d)).

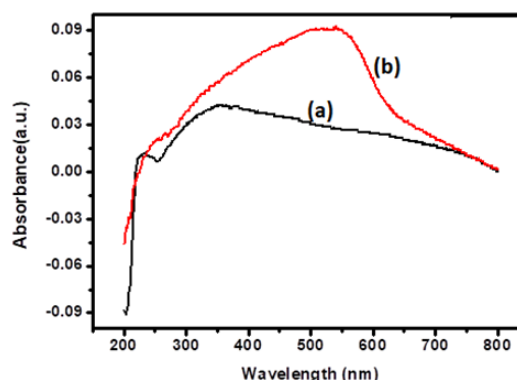


Fig. 3. UV-Vis DRS spectra of prepared nanoparticles

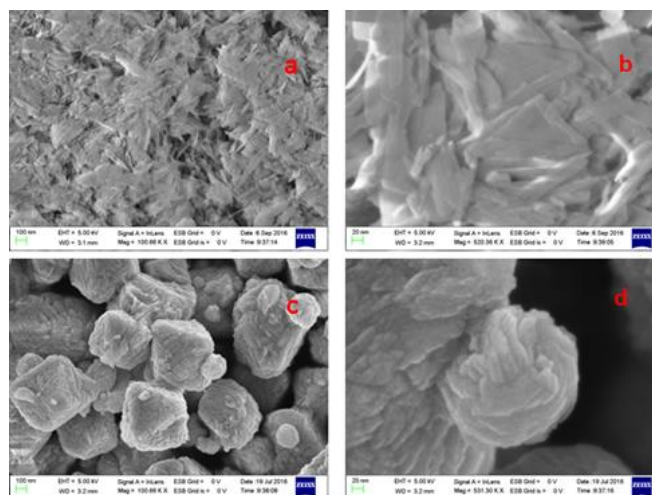


Fig. 4. FESEM images of (a,b) CuO NPs and (c,d) Cu₂O NPs

EDS spectra of the CuO NPs and Cu₂O NPs are presented in Figure 5. The presence of copper (Cu) and oxygen (O) in CuO NPs and Cu₂O NPs confirms the formation of CuO NPs and Cu₂O NPs.

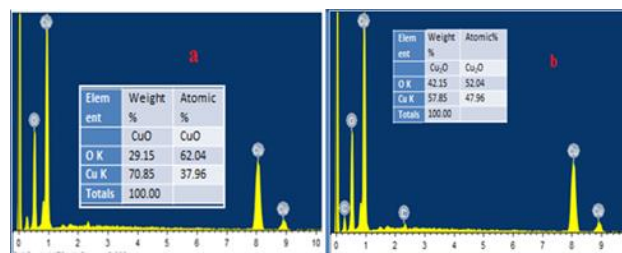


Fig. 5. EDS spectra of CuO NPs (a), and Cu₂O NPs (b)

4. Conclusion

In this research study, CuO NPs and Cu₂O NPs were successfully synthesized by sonochemical method using copper acetate as precursor at different reducing agents. The XRD and FTIR results confirmed formation of the CuO NPs and Cu₂O NPs. Bandgap of the CuO NPs and Cu₂O NPs were 2.38 and 1.82, respectively. In addition, it was found that the phase purity was critically depend on the reducing agents.

Conflict of interest

The authors clearly declared that they have no any conflict of interest.

References

- [1] a) Yang F, Tang Q, Zhong X. *Int J. Nanomedicine*, 2012, **7**:835 b) A. Hameed, G.R. Fatima, K. Malik, A. Muqadas, M. Fazal-ur-Rehman, *J. Med. Chem. Sci.*, 2019, **2**: 9 c) A. Mirzaie, *J. Med. Chem. Sci.*, 2018, **1**:5 d) S. Gupta, M. Lakshman, *J. Med. Chem. Sci.*, 2019, **2**: 51
- [2] Lee P, Zhang R, Li V. *Int J. Nanomedicine*, 2012, **7**:731
- [3] Murphy E. A, Majeti B. K, Barnes L. A. *Proc Natl Acad Sci USA*, 2008, **105**:9343
- [4] Siddiqui I. A, Adhami V. M, Christopher J, Chamcheu, Mukhtar H. *Int J Nanomedicine*, 2012, **7**:591
- [5] a) Stevens M. M, Ghadiali J. E, Cohen B. E. *ACS Nano*, 2010, **4**:4915 b) M. Soleiman-Beigi, Z. Arzehgar, Synlett, 2018, 29:986 c) S. Sajjadifar, Z. Arzehgar, S. Khoshpoori, J. Inorg. Organomet. Polym. Mater., 2018, 28:837 d) Z. Arzehgar, S. Sajjadifar, H. Arandiyani, *Asian J. Green Chem.*, 2019, **3**:43 e) Z. Arzehgar, S. Sajjadifar, M. Fekri, *Chem. Methodol.*, 2019, **3**: 251 f) S. Sajjadifar, Z. Arzehgar, A. Ghayuri, *J. Chin. Chem. Soc.*, 2018, **65**:205 g) Z. Arzehgar, A. Aydi, M. Mirzaei Heydari, *Asian J. Green Chem.*, 2018, **2**:281
- [6] Shrestha K M, Sorensen C M and Klabunde K J, *J. Phys. Chem. C*, 2010, **114**: 14368
- [7] Yin M, Wu C K, Lou Y, Burda C, Koberstein J T, Zhu Y and O'Brien S, *J. Am. Chem. Soc.* 2005, **127**, 9506
- [8] a) V. V. T. Padil, M. Černík, *Int. J. Nanomed.* 2013, **8**:889 b) I. Sheikhshoaei, S. Davary, S. Ramezanzpour, *Chem. Methodol*, 2018, **2**:47
- [9] G. Ren, D. Hu, E. W Cheng, M. A. Vargas-Reus, P. Reip, R. P. Allaker, *Int. J. Antimicrob. Agents*, 2009, **33**: 587
- [10] C. T. Hsieh, J. M. Chen, H. H. Lin, H. C. Shih, *Appl. Phys. Lett.*, 2003, **82**: 3316
- [11] X. Zhang, G. Wang, X. Liu, *J. Phys. Chem. C Nanomater. Interfaces*, 2008, **112**: 16845
- [12] L. Huang, F. Peng, H. Yu, H. Wang, *Mater. Res. Bull.*, 2008, **43**:3407
- [13] H. S. Shin, J. Y. Song, J. Yu, *Mater. Lett.*, 2009, **63**:397
- [14] C. Shu-Jian, C. Xue-Tai, Z. Xue, L. Li-Hong, Y. Xiao-Zeng, *J. Cryst. Growth.*, 2002, **246**:169
- [15] C. Y. Wang, Y. Zhou, Z. Y. Chen, B. Cheng, H. J. Liu, X. Mo, *J. Colloid Interface Sci.*, 1999, **220**: 468
- [16] B. Miljevic, F. Hedayat, S. Stevanovic, K. E. Fairfull-Smith, S. E. Bottle, Z. D. Ristovski, *Aerosol Sci. Tech*, 2014, **48**:1276
- [17] Y. C. Zhang, J.Y. Tang, Wang, G.L. Zhang, M. Hu, X.Y. J. *Cryst. Growth*, 2006, **294**:278
- [18] I. Prakash, P. Muralidharan, N. Nallamuthu, M. Venkateswarlu, N. Satyanarayana, *Mater.Res. Bull.*, 2007, **42**:1619
- [19] Z. Zhang, *ACS Nano*, 2013, **7**:1709
- [20] X. Guo, P. Diao, D. Xu, S. Huang, Y. Yang, T. Jin, M. Zhang, 2014, *Int. J. Hydrogen Energy*, **39**:7686